

1275. Effect of grinding wheel on the dynamic performance of high-speed spindle system with an improved FE model

Zhouping Wu¹, Beizhi Li², Jianguo Yang³, Steven Liang⁴

^{1,2,3}Advanced Manufacturing Center of Donghua University, Shanghai, China

⁴Georgia Institute of Technology, Atlanta, USA

²Corresponding author

E-mail: ¹wuzhouping1984@126.com, ²beizhili@aliyun.com, ³jgyangm@dhu.edu.cn,

⁴steven.liang@me.gatech.edu

(Received 29 October 2013; received in revised form 12 February 2014; accepted 5 March 2014)

Abstract. The grinding wheel is a key factor which should be considered in the process of predicting the dynamic performance of the high-speed spindle system. Currently, most research is mainly focuses on shaft and bearing using Timoshenko's beam and Jones' bearing model. In this research, considering the effect of grinding wheel on the dynamic behavior of the high-speed motorized spindle system, a dynamic model of spindle system has been established by utilizing the finite element method (FEM). The model is improved by optimizing the relevant parameters of spindle system and validated by measuring FRF using impact hammer test. The reported results are well matched (maximum error is 5 %). Using the improved model, the effect of grinding wheel on the critical speeds, mode shapes, centrifugal force and gyroscopic effects of spindle system are analyzed. In addition, the impact of different diameters, materials and fixed methods of grinding wheel on the dynamic property of spindle system are also carried out. The result shows the affect of grinding wheel and design guideline of the spindle and grinding wheel.

Keywords: grinding wheel, dynamic performance, high-speed spindle system, improved FE model.

1. Introduction

High-speed machining (HSM) technology has been widely used in aerospace, automotive, electronics and many other industries to increase efficiency and reduce production costs. This technology is mainly limited by the dynamic performance of the spindle system, which has a great influence on the machining accuracy [1]. So it is important to accurately obtain the dynamic performance of the high-speed spindle system.

Early spindle research mainly studied the dynamic characteristic of bearing-shaft system through different theory and FEM methods [2-4]. Ruhl [5] was one of the earliest researchers who use the finite element method (FEM) to model rotor systems for predicting the stability and unbalanced response. His model included translational inertia and bending stiffness, but neglected rotational inertia, gyroscopic moments, shear deformation and axial load. Nelson [6] employed the Timoshenko beam theory to establish the system matrices for analyzing the dynamics of rotor systems with the effects of rotary inertia, gyroscopic moments, shear deformation, and axial load. The bearings are modeled as linear springs. Chen et al. [7] presented a model which contains the spindle and the bearings to determine the response of a spindle system at high speeds by applying an analytical method. Current research is expanded to model the spindle system to gain the dynamic property of the spindle system by combining simulation with experiment [8-10]. The general models outlined by Yusuf Altintas [11] and Shuyun Jiang [12], which consist of spindle shaft, angular contact ball bearings and housing, have been experimentally verified. But these studies neglected the dynamic affect of the machine tool. Yuzhong Cao [13] presented a integrated model of the spindle-bearing and machine tool system to predict mode shapes, frequency response function (FRF), static and dynamic deflections along the cutter and spindle shaft. A dynamic high-speed spindle system model, which includes the drilling head, is elaborated by F. Forestier [14] on the basis of rotor dynamics predictions and validated by comparing the numerical FRF

with experimental results.

However, the research about the effect of grinding wheel which plays an important role in the dynamic performance of high-speed spindle system is rarely studied. This study sets up an improved finite element model of spindle system which contains the shaft, bearings, rotor and grinding wheel to analyze the effect of grinding wheel. The shaft and rotor are modeled as Timoshenko's beam by including the centrifugal force and gyroscopic effects. The bearing is modeled as Jones' bearing model that includes the centrifugal force and gyroscopic effects from the rolling elements of bearings. The grinding wheel is modeled as a rigid disk which is fitted on the shaft by bolts. The finite element model was validated and improved by measuring FRF using impact hammer test. The reported results show that the accuracy of improved model increase by 10 % compared with the initial one. Through the improved model, the dynamic performance of the spindle system is studied. The effect of grinding wheel on the critical speeds, mode shapes, centrifugal force and gyroscopic effects of spindle system are analyzed. And, the effect of different diameter, material and fixed method of grinding wheel on the dynamic property of spindle system were also carried out. The result shows the affect of parameter and fixed method of grinding wheel and design guideline of the spindle and grinding wheel.

2. Spindle model

2.1. Structure of the high-speed spindle system

The high-speed spindle system with a maximum rotating speed of 11000 rpm experimentally, is shown as Fig. 1. It is mainly composed of spindle (include shaft, rotor, bearings) and grinding wheel and other major component parts with rated power 41.5 kW. The material of the shaft is 42 CrMo; ceramic, silicon sheet and 45 steel are respectively used for bearings, rotor and other parts. The CBN type grinding wheel, whose basal body is made of 45 steel, is fitted on the shaft by 12 bolts in circumferential array. The shaft is supported by the preloaded bearings, i.e. two pairs of parallel front bearings and one pair of parallel rear bearings. Here, the type of front bearings is HCB71924-E-P4S and the rear bearings' type is HCB71913-E-T-P4S. The preload of the front bearings is 212 N, while 55 N for the rear bearings.

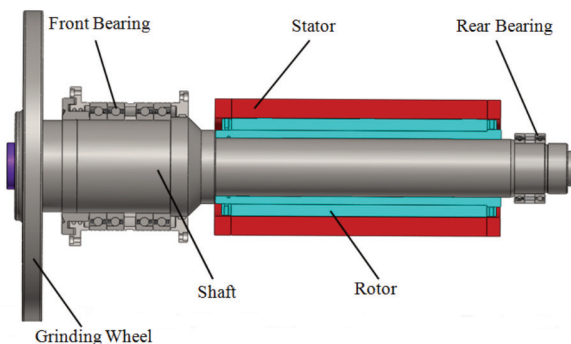


Fig. 1. Structure of the high-speed spindle system

2.2. Equations of motion of spindle and grinding wheel

Due to the size of the rotor portion of spindle (include shaft and rotor), shear deformations must be taken into account. The Timoshenko beam theory which includes the shear deformations (θ_x in Fig. 2) and rotational inertia effects is used to model the rotor portion, making it suitable for describing the behavior of shaft and rotor. Dynamic equations were obtained by using Lagrange formulation associated with a numerical finite element method.

The motion of each FE node is described by three translational ($\delta_x, \delta_y, \delta_z$) and two rotational

(γ_x, γ_y) degrees of freedom:

$$\{q\} = \{\delta_x, \delta_y, \delta_z, \gamma_x, \gamma_y\}. \tag{1}$$

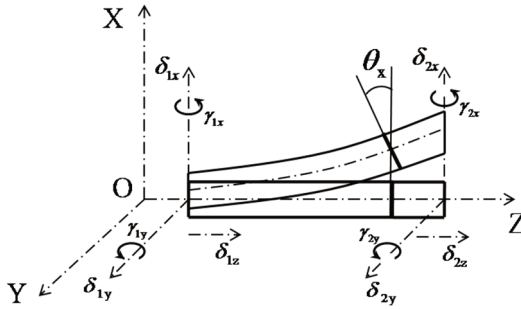


Fig. 2. Timoshenko beam degrees of freedom

Considering the centrifugal and gyroscopic effects, the equations of motion of the rotor portion can be attained in matrix forms by using Lagrange’s equations associated with the FE method [11]:

$$[M]_b \{\ddot{x}\} - \Omega [G]_b \{\dot{x}\} + ([K]_b - \Omega^2 [M]_c) \{x\} = \{F(t)\}_b + \{P\}_b, \tag{2}$$

where $[K]_b$ and $[M]_b$ are the stiffness and mass matrices of rotor portion, $[G]_b$ is the skew-symmetric gyroscopic matrix, $[M]_c$ is the mass matrix for computing the centrifugal force, Ω is the rotating speed, $\{F(t)\}_b$ and $\{P\}_b$ are the external exciting force vector (e.g. cutting force) and constant load force (e.g. gravity force).

The grinding wheel mounted on the front of shaft is modeled as a rigid disk, and the equation of motion is:

$$[M]_g \{\ddot{x}\} - \Omega [G]_g \{\dot{x}\} = \{F(t)\}_g + \{P\}_g, \tag{3}$$

where $[M]_g$ is the mass matrix of grinding wheel, $[G]_g$ is the gyroscopic matrix, $\{F(t)\}_g$ and $\{P\}_g$ are the external exciting force vector and constant load force.

2.3. Rolling bearing model

The spindle shaft is supported by six ball angular contact bearings. The Jones’ bearing model [15], which considers both centrifugal and gyroscopic effects on the balls, is used. When the high-speed spindle system operating at high speed, equation of deformation of the bearing under the load from the rotor can be expressed as:

$$\begin{Bmatrix} F_x \\ F_y \\ F_z \\ M_x \\ M_y \end{Bmatrix} = \begin{bmatrix} k_{\delta_x \delta_x} & k_{\delta_x \delta_y} & k_{\delta_x \delta_z} & k_{\delta_x \gamma_x} & k_{\delta_x \gamma_y} \\ k_{\delta_y \delta_x} & k_{\delta_y \delta_y} & k_{\delta_y \delta_z} & k_{\delta_y \gamma_x} & k_{\delta_y \gamma_y} \\ k_{\delta_z \delta_x} & k_{\delta_z \delta_y} & k_{\delta_z \delta_z} & k_{\delta_z \gamma_x} & k_{\delta_z \gamma_y} \\ k_{\gamma_x \delta_x} & k_{\gamma_x \delta_y} & k_{\gamma_x \delta_z} & k_{\gamma_x \gamma_x} & k_{\gamma_x \gamma_y} \\ k_{\gamma_y \delta_x} & k_{\gamma_y \delta_y} & k_{\gamma_y \delta_z} & k_{\gamma_y \gamma_x} & k_{\gamma_y \gamma_y} \end{bmatrix} \cdot \begin{Bmatrix} \delta_x \\ \delta_y \\ \delta_z \\ \gamma_x \\ \gamma_y \end{Bmatrix}, \text{ or } F = K\delta, \tag{4}$$

where F is force vector on the bearing from rotor, K and δ are stiffness and deformation matrix of bearing. Here the stiffness of bearing in γ_x and γ_y free degrees are not considered for their minimal impact. The stiffness of bearing in δ_x , δ_y and δ_z free degrees are obtained by derivative F in corresponding deformation.

By assembling equations of the grinding wheel, rotor portion and bearing, the following

general nonlinear dynamic equations of the spindle system can be obtained:

$$\begin{aligned}
 [M]\{\ddot{x}\} + [C]\{\dot{x}\} + [K]\{x\} &= \{F(t)\}, \\
 [M] &= [M]_b + [M]_g, \quad [C] = -\Omega([G]_b + [G]_g) + [C^s], \\
 [K] &= [K]_b - \Omega^2[M]_c + K, \quad \{F(t)\} = \{F(t)\}_b + \{F(t)\}_g + \{P\},
 \end{aligned}
 \tag{5}$$

where $[C^s]$ is the structural damping which should be obtained from experimental modal analysis.

The motion of spindle system is considered as the superposition of rigid and elastic body displacements. The dynamic spindle system model is built up by coupling the rotor portion, grinding wheel and bearing by using finite element method (Fig. 3). The small holes, small shaft shoulders and angle of chamfers are neglected in this model to simplify the FE model of spindle system. The interfaces between shaft and rotor, shaft and inner rings of bearings are assumed to be rigid. In order to get better accuracy, the mesh size of grinding wheel and shaft are much smaller than other parts. The spider node (orange point) which rigidly connects every node of inner rings represents the inner ring of bearing. The outer ring of bearing is fixed in the housing and assumed to be completely restraint (shown in A-A in Fig. 3). The balls of bearing are treated as springs in X, Y and Z directions. The 12 bolts between the grinding wheel and shaft are treated as beams (show in the bottom picture of Fig. 3).

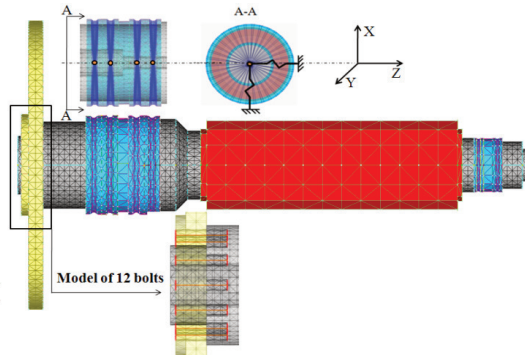


Fig. 3. Finite-element model of the high-speed spindle system

3. Experimental characterization and model improvement

Because of the geometrical and physical complexity, the material properties of the spindle and the grinding wheel cannot be precisely known. The eccentricity (δ) should be defined when analyze the dynamic performance of the spindle system. The recognition of the damping which represents the dissipative properties in Eq. (5) is important to improve the model of the spindle system.

An improved procedure is proposed to adjust the variable above in order to make the model consistent with experimental. Least-squares type object function is used when updating the parameters. The optimization goal is minimizing the gap between the measured and analyzed acceleration of grinding wheel node FRF (frequency response function) (Fig. 4). Process of experimental determination of the dynamic characteristics of the spindle system is carried out by an impact hammer test (Fig. 5). The accelerated speed of the front shaft node was recorded using an accelerometer (sensitive of 100 mv/g, frequency range of 0.5-6000 Hz). The impact hammer is hammered on the grinding wheel in $-Y$ direction. The signals from the accelerometer and the hammer are collected by LMS whose measurement frequency range is set from 0 to 1080 Hz.

The Rayleigh viscous equivalent damping which makes it possible to regard the damping matrix $[C^s]$ as a linear combination of the mass matrix \mathbf{M} and the rigidity matrix \mathbf{K} is used to modeling the damping of the spindle system. The mass matrix \mathbf{M} is the mass of spindle. The

rigidity matrix \mathbf{K} contains the spindle rigidity matrix \mathbf{K} of spindle and the rolling bearing rigidity matrix \mathbf{K} of bearing.

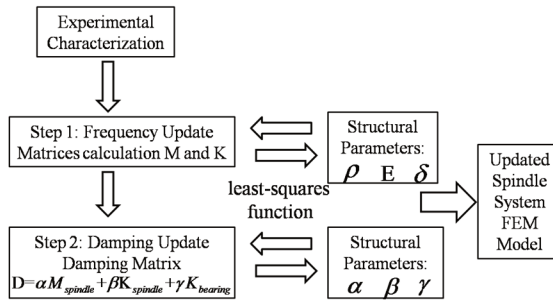


Fig. 4. Procedure of numeric model update

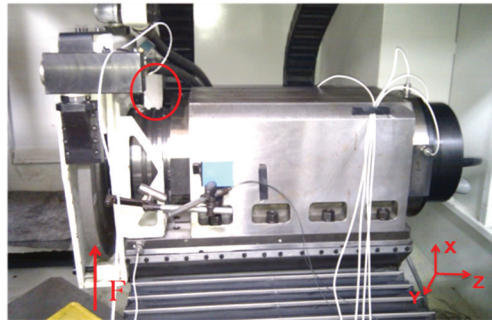


Fig. 5. Experimental set up

Initial and updated value of the parameters above is show in Table 1. For the rotor portion, the updated ρ is larger and E is smaller because the numeric model is simplified by ignoring holes, small shoulder.

Table 1. Initial and updated parameters of spindle system

Parameters	ρ (kg/m ³)		E (Pa)	δ (μ m)	α	β	γ
Initial Value	Shaft	7850	2.11E10 ¹¹	0.4	0.5	0.2	0.2
	Grinding Wheel	7850	2.11E10 ¹¹				
Updated Value	Shaft	8023	1.97E10 ¹¹	1	0.673	0.109	0.073
	Grinding Wheel	7802	2.02E10 ¹¹				

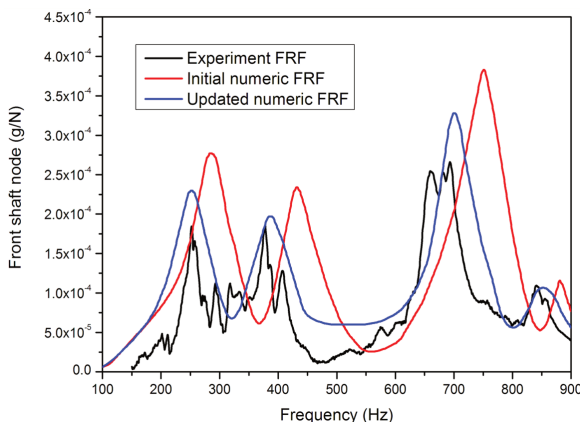


Fig. 6. Experimental, initial and updated FRF of front shaft node

For the grinding wheel, the updated ρ and E are both smaller because the material of whole part of grinding wheel is regarded as steel in initial model. The initial δ is eccentricity without grinding wheel from direction of spindle. The improved δ is measured by SBS. The initial value of α , β , γ are defined by experience and improved by LMS. The front shaft node FRF from the numeric model and experiment are show in Fig. 6. The improved analysis result generates a good correspondence in a bandwidth of 200-900 Hz. The maximum error of the improved model is about 5 %, while it is about 15 % for the initial model.

4. Dynamic analysis

Based on the updated model above, the FEMAP with Nastran is used to analyze the dynamic performance of the High-speed grinding motorized spindle system. The parameters of the high-speed motorized spindle are listed in Table 2.

Table 2. Parameters of the spindle system

Length of the spindle	715 mm
Front bearing	HCB71924
Axial preload of front bearing	212 N
Rear bearing	HCB71913
Axial preload of rear bearing	55 N
Diameter of the grinding wheel	400 mm
Maximum rotating speed of the spindle	10000 rpm

4.1. Dynamic performance analysis

For a rotor system, when the system rotates at the speeds equal to its synchronous whirl frequencies, it will resonate due to the amount of residual unbalance which could not be avoided in manufacturing and assembling; these speeds are defined as critical speeds. In this study, the first four critical speeds are 15300, 23400, 42000 and 51000 rpm, respectively; and corresponding mode shapes are given in Table 3. It is shown in Table 3 that the first mode shape is located at the front of shaft and grinding wheel, which will greatly affect the accuracy of machining; the second is mainly the twisted mode of the grinding wheel around Y axis and bending mode of the rotor; the third is twisted mode of the grinding wheel around X axis; and the fourth is the bending mode of the grinding wheel. So the grinding wheel is a sensitive part to impact the dynamic behavior of the spindle system.

The simulated dynamic stiffness from the FE model at the front shaft node of different rotational speeds is shown in Fig. 7. It shows that the dynamic stiffness of the spindle system decreases with the increase of rotation speed because of the rise of centrifugal force and gyroscopic moment. When the spindle rotates at the maximum working speed (10000 rpm), the dynamic stiffness is about 93 % of the static stiffness.

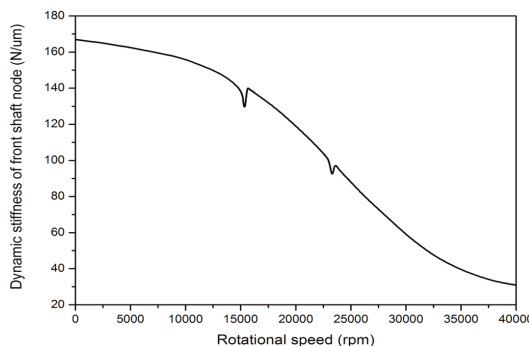


Fig. 7. Simulated dynamic stiffness at the spindle nose

Fig. 8 shows an impact force which is applied on the front shaft node in the radial direction. The impact force which is 100 N changes as sine function and lasts 0.005 s (shown in Fig. 8(a)). The radial displacement time response histories of the different parts of spindle system are shown in Fig. 8(b). The grinding wheel node has the largest amplitude which is 8.5×10^{-7} m. After 0.0225 s, the amplitude decreases to less than 0.5×10^{-7} m. The amplitude of middle shaft node is 2×10^{-7} m and reduces to less than 0.5×10^{-7} m after 0.0113 s. The rear shaft node has the smallest amplitude which is 0.7×10^{-7} m, and the amplitude only needs 0.0075 s to reach less than 0.5×10^{-7} m. From the analysis above it can be seen that the grinding wheel is the most sensitive part of the high-speed spindle system for impact force.

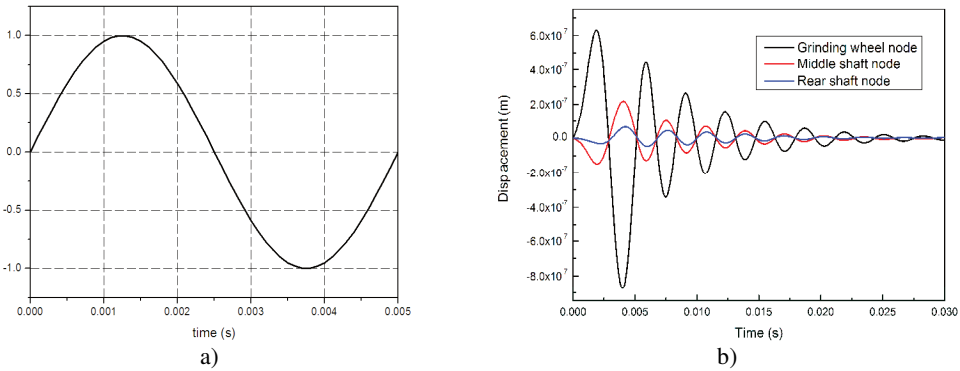


Fig. 8. Impact response in the radial direction at different part of the spindle system: 200 Hz sine function a) and b) radial displacement time response histories

4.2. Comparison and discussion

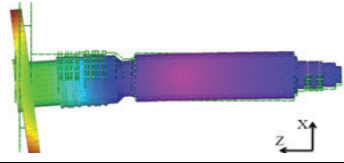
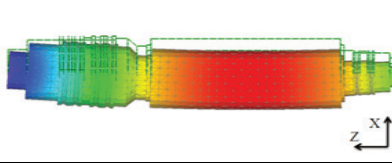
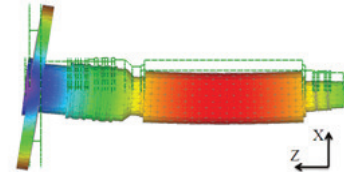
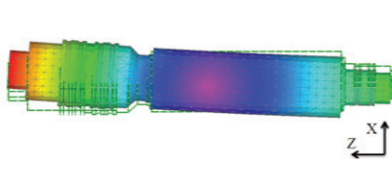
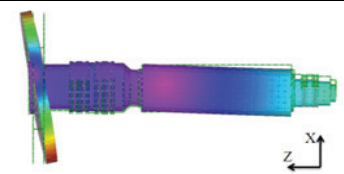
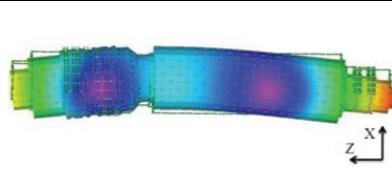
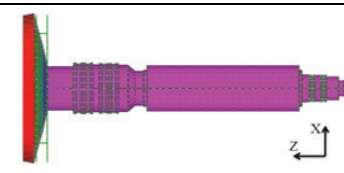
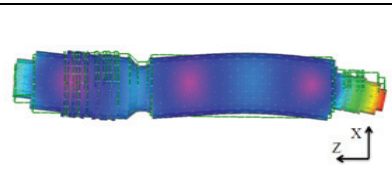
To obtain the effect of grinding wheel on the dynamic performance of the spindle system, a comparative study has been done between the spindle system with and without grinding wheel. The first four critical speeds and their corresponding mode shapes of spindle system with and without grinding wheel are listed in Table 3. It can be seen that the first critical speed of spindle system without grinding wheel is 28260 rpm. It is much higher than the critical speed of spindle system with grinding wheel, which is only 15300 rpm. The second to fourth critical speeds of spindle system without grinding wheel is 54060, 123180 and 135900 rpm, respectively. These critical speeds are also much higher than the corresponding speeds of spindle system with grinding wheel.

The first mode shape of the spindle system without grinding wheel is mainly located at the rotor which is in the middle of the spindle system. Compared with the spindle system with grinding wheel, this model shape will not affect the accuracy of machining directly. The second mode shape is the bending mode of the shaft in the front of the spindle system. The third is the bending mode of both the front and rear part of the shaft and the fourth is the bending mode for the front, rear and middle part of the shaft. These critical speeds and mode shapes are quite different to the spindle system with grinding wheel. In summary, the grinding wheel has great influence on the critical speeds and mode shapes.

In order to check the influence of centrifugal force and the gyroscopic moment of the spindle system on critical speeds, a comparative analysis has been done between the spindle system with and without grinding wheel. Fig. 9 shows the rotation effects from the spindle system with and without grinding wheel on critical speeds. Both the centrifugal forces and gyroscopic moments have a greater influence on the first critical speed of the spindle system with grinding wheel than without grinding wheel. For the spindle system with grinding wheel, the gyroscopic moments affect more than the centrifugal forces, for example, at the speed of 30,000 rpm, the first critical speed drops 9.8 % and 11.8 % due to the centrifugal forces and gyroscopic moments, respectively.

While for the spindle system without grinding wheel, the gyroscopic moments affect less than the centrifugal forces, such as, at the speed of 30.000 rpm, the first critical speed drops 4.5 % and 2.8 % due to the centrifugal forces and gyroscopic moments, respectively.

Table 3. Critical speeds and mode shapes of spindle system with and without grinding wheel

1st		1st	
15300 rpm		28260 rpm	
2nd		2nd	
23400 rpm		54060 rpm	
3rd		3rd	
42000 rpm		123180 rpm	
4th		4th	
51000 rpm		135900 rpm	

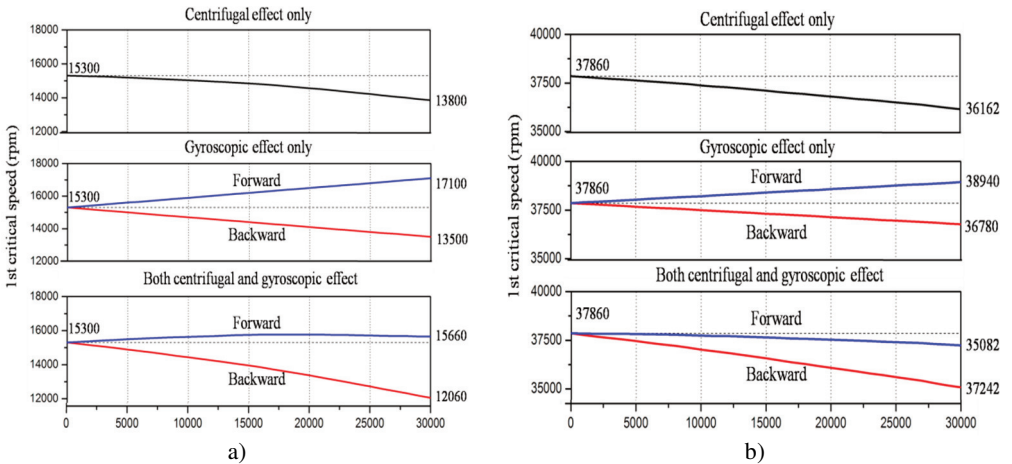


Fig. 9. Rotation effect on first critical speeds: with grinding wheel a) and b) without grinding wheel

The critical speeds of spindle system with different diameter, material and installation mode have been analyzed to further study the effect of grinding wheel on the dynamic performance of the spindle system. The diameter is from 200 to 500 mm, the materials of basal body of grinding wheel are 45 steel and Al. The installation modes are shown in Fig. 10. Additionally, the material of the second installation modes is configured for 45 steel (Fig. 10(b)).

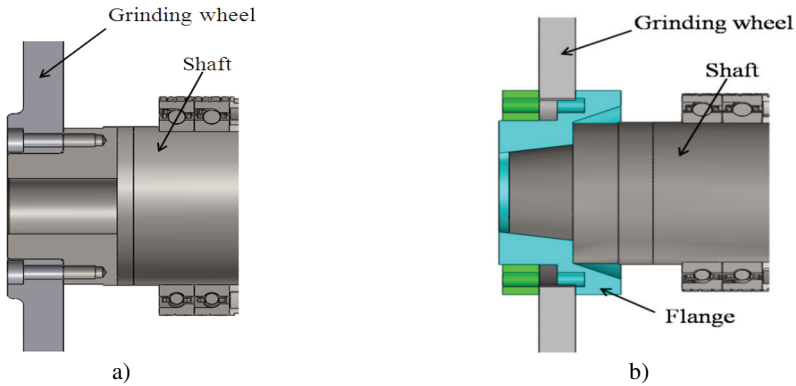


Fig. 10. Different installation modes of grinding wheel: without flange a) and b) with flange

Fig. 11 shows the first four critical speeds of the spindle system with different diameter, material and installation modes of the grinding wheel. The horizontal axis is the diameter of the grinding wheel. The vertical axis is the critical speeds of the spindle system. The black line stands for the critical speed of spindle system with steel basal body grinding wheel. The red line expresses the critical speed of spindle system with Al basal body grinding wheel. The blue line is the critical speed of spindle system with the second installation mode. For the 1st critical speed (Fig. 11(a)), all the three lines decrease as the diameters of the grinding wheel increase. The black and red line fall slowly within 375 mm and go down quickly without 375 mm. Besides, the red line is always above the black line. The blue line falls down sharply between 275 mm and 450 mm.

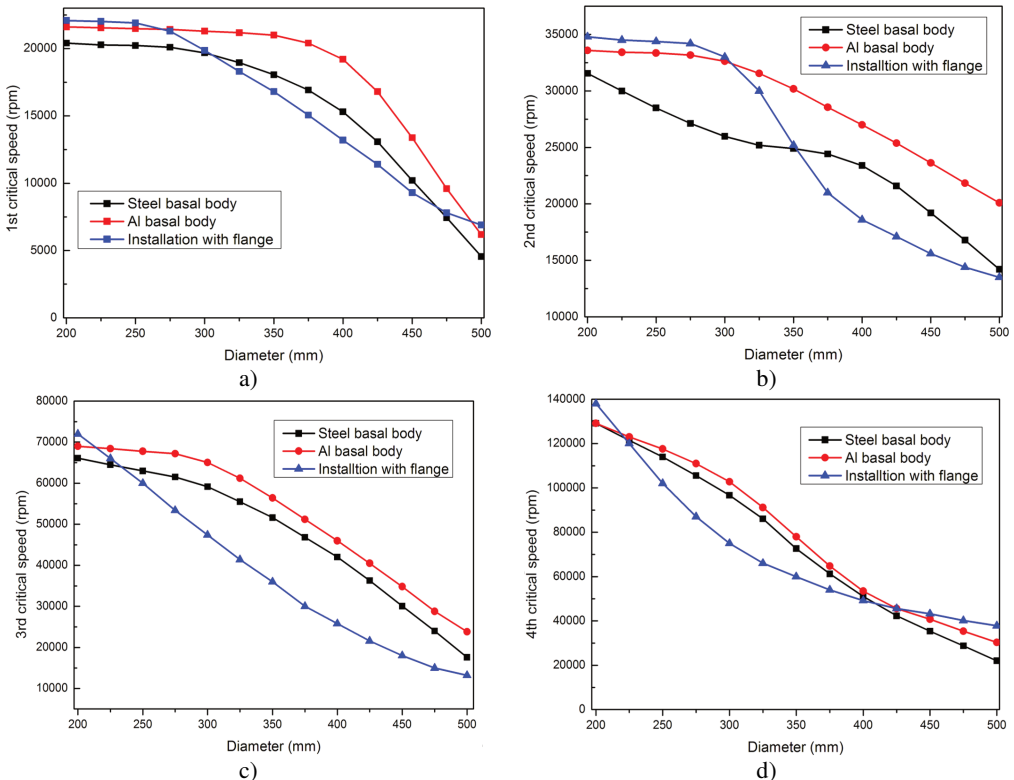


Fig. 11. First four critical speeds of the spindle system: a) 1st critical speed, b) 2nd critical speed, c) 3rd critical speed and d) 4th critical speed

For the 2nd, 3rd and 4th critical speeds, the decrease of red lines are accordant with the 1st critical speed. The black line in Fig. 11(b) falls down quickly within 300 mm and beyond 400 mm, while between 300 mm and 400 mm it falls smoothly. The black lines in Fig. 11(c) and Fig. 11(d) have the same trend as the Fig. 11(a). The changing trend of the two blue lines in Fig. 11(b) and Fig. 11(a) are accordant. The blue lines in Fig. 11(c) and Fig. 11(d) are also nearly the same.

In summary, these four critical speeds of spindle system decrease as the increase of the diameters of the grinding wheel. The four critical speeds of the spindle system with Al basal body grinding wheel is always higher than the spindle system with steel basal body grinding wheel. For the second installation mode of grinding wheel, the dynamic performance is better than the first installation mode in some range, because the effect from flange changes as the diameters of grinding wheel increase. When the diameter is small, the mode shape is mainly located at the middle of shaft. The installation of flange increases the stiffness of the spindle system. So the second installation has better dynamic performance in this case. While as the diameter rises up, the mode shape transfers to the grinding wheel. The dynamic performance of the spindle system without flange is better because of the larger stiffness of the connection. When the grinding wheel is larger than 500 mm, it will be very flexible. In this situation, the flange will increase the stiffness because of larger connect surface. For this spindle system whose grinding wheel fitted on the shaft directly without flange, its dynamic performance is better when the diameter of grinding wheel is 400 mm.

5. Conclusion

In this paper, an integrated finite element model (FEM) of high-speed motorized spindle system which contains the grinding wheel is developed. The FEM is verified and updated experimentally to characterize the dynamic behavior of the spindle system. With the updated model, the dynamic performance of spindle system and the effect of grinding wheel on the dynamic performance of spindle system are analyzed. The results showed that:

1. The dynamic stiffness of the spindle system decreases as the rotation speed increases because of the centrifugal force and gyroscopic moment. The grinding wheel node is the most sensitive part to the exciting force.
2. The grinding wheel has a great effect on the critical speeds and their corresponding mode shapes of the spindle system. The grinding wheel should be taken in to account when analyzing the critical speeds and their corresponding mode shapes of the high-speed spindle system.
3. The spindle system with grinding wheel has larger centrifugal force and gyroscopic moment than without grinding wheel. For the spindle system with grinding wheel, the gyroscopic moments affect more than the centrifugal forces. For the spindle system without grinding wheel, it is opposite.
4. The spindle system with Al basal body grinding wheel has higher critical speed than the spindle system with steel basal body grinding wheel when the diameter of grinding wheel is same. In the diameter range of 300 mm to 400 mm, the installation mode without the flange has better performance.

Acknowledgement

This paper is supported by Major National Science and Technology Project (2011ZX04016-041-DH01).

References

- [1] **Zhouping Wu, Beizhi Li, Jianguo Yang, Xia Sheng** A thermodynamics coupled modeling approach for analysis and improvement of high-speed motorized spindle system. *Journal of Vibroengineering*, Vol. 15, Issue 3, 2013.

- [2] **Harkany** The determination of the optimum bearing distance with regard to bearing stiffness in the case of shafts with constant and variable cross sections, respectively. *Machine Tool Industry Research Association Translation*, Vol. 33, 1961, p. 103-117.
- [3] **Opitz H., Gunther D., Kalkert W., Kunkel H.** The study of the deflection of rolling bearing for machine tool spindles. *Proceeding of the 6th MTDR Conference*, Vol. 34, 1965, p. 257-269.
- [4] **Vincent Gagnol, Thien-PhuLe, Pascal Ray** Modal identification of spindle-tool unit in high-speed machining. *Mechanical Systems and Signal Processing*, Vol. 25, 2011, p. 2388-2398.
- [5] **Ruhl R. L., Booker J. F.** A finite element model for distributed parameter turbo rotor systems. *ASME Journal of Engineering for Industry*, 1972, p. 128-139.
- [6] **Nelson H. D.** A finite rotating shaft element using Timoshenko beam theory. *ASME Journal of Mechanical Design*, Vol. 102, Issue 4, 1980, p. 793-803.
- [7] **Chen C. H., Wang K. W., Shin Y. C.** An integrated approach toward the dynamic analysis of high-speed spindles, Part I: system model; Part II: dynamics under moving end load. *International Journal of Vibration and Acoustics*, Vol. 116, Issue 4, 1994, p. 506-522.
- [8] **Gagnol V., Bouzgarroua B. C., Raya P., Barra C.** Model-based chatter stability prediction for high-speed spindles. *International Journal of Machine Tools and Manufacture*, Vol. 47, 2007, p. 1176-1186.
- [9] **Hongrui Cao, BingLi, Zhengjia He** Chatter stability of milling with speed-varying dynamics of spindles. *International Journal of Machine Tools and Manufacture*, Vol. 52, 2012, p. 50-58.
- [10] **Sun-Min Kim, Jae-Hoon Ha, Sung-Ho Jeong, Sun-Kyu Lee** Effect of joint conditions on the dynamic behavior of a grinding wheel spindle. *International Journal of Machine Tools and Manufacture*, Vol. 41, 2001, p. 1749-1761.
- [11] **Yuzhong Cao, Yusuf Altintas** A general method for the modeling of spindle-bearing systems. *Journal of Mechanical Design*, 2004, p. 26-134.
- [12] **Shuyun Jiang, ShufeiZheng** A modeling approach for analysis and improvement of spindle-drawbar-bearing assembly dynamics. *International Journal of Machine Tools and Manufacture*, Vol. 50, 2010, p. 131-142.
- [13] **Yuzhong Cao, Altintas Y.** Modeling of spindle-bearing and machine tool systems for virtual simulation of milling operations. *International Journal of Machine Tools and Manufacture*, Vol. 47, 2007, p. 1342-1350.
- [14] **Forestier F., Gagnol V., Ray P., Paris H.** Model-based operating recommendations for high-speed spindles equipped with a self-vibratory drilling head. *Mechanism and Machine Theory*, Vol. 46, 2011, p. 1610-1622.
- [15] **Jones A. B.** A general theory for elastically constrained ball and radial roller bearings under arbitrary load and speed conditions. *ASME J. Basic Eng.*, p. 309-320.